Solar Energy Materials & Solar Cells 94 (2010) 930–934

Contents lists available at ScienceDirect

Solar Energy Materials & Solar Cells

journal homepage: www.elsevier.com/locate/solmat

Letter

Growth of vertically aligned ZnO nanorod arrays as antireflection layer on silicon solar cells

J.Y. Chen, K.W. Sun *

Department of Applied Chemistry, National Chiao Tung University, Hsinchu, Taiwan

ARTICLE INFO

Article history:
Received 26 November 2009
Accepted 4 January 2010
Available online 22 January 2010

Keywords:
Nanorod array
Antireflection
Solution synthesis

ABSTRACT

In this work we investigated the effects of growth time, spin-coating rates, and solution concentration on the reflection properties of the solution-grown ZnO nanorod arrays. The vertically aligned nanorod arrays were deposited on the surface of the Si solar cells as the antireflection (AR) layer. We found that the nanorod morphology, controlled through synthetic chemistry, has a great effect on the AR layer performance. We also demonstrated that the light harvest efficiency of the solar cells was greatly improved from 10.4% to 12.8% by using the vertically aligned ZnO nanorod arrays as the AR layer on poly-Si solar cells.

© 2010 Elsevier B.V. All rights reserved.

1. Introduction

An antireflection (AR) layer is a type of coating applied to the surface of a material to reduce light reflection and to increase light transmission. The AR layers can be used in solar cells, planar displays, glasses, prisms, videos, and camera monitors. Surface-relief gratings with the sizes smaller than the wavelength of light, named subwavelength structures (SWSs), behave as AR surfaces. By using a mechanically continuous wavelike grating (e.g., pyramidal, triangular, and conical shapes), the SWS grating acts as a surface possessing a gradually and continuously changing refractive index profile from the air to the substrate. Deeper SWS gratings can greatly enhance the AR effect, since the refractive index value changes smoothly and continuously. Tapered SWSs have been fabricated through different methods [1–9]. Ishimori et al. used an e-beam lithography technique to generate triangular structures in the photoresist and utilized a focused SF_6 fast atom beam (FAB) to produce tapered SWSs. However, the fabrication costs, which involve either electron-beam lithography or various etching processes, can be significant. Recently, versatile SWSs have emerged as promising candidates for AR coatings such as etching with self-aggregated nanodot mask [4,5], moth-eye-like fabrication [6,7], and nanostructures employing oblique-angle deposition methods [8,9].

More recently, ZnO becomes attractive as a dielectric AR layer material because of its good transparency, appropriate refractive index, and ability to form textured coating via anisotropic growth [10–17]. Various physical, chemical, and electrochemical deposition techniques have been explored to create oriented arrays of ZnO nanorod. For instance, pulsed laser deposition [10], metal-organic chemical vapor deposition [11], and epitaxial electrodeposition [12] have been achieved in the fabrication of ZnO nanorod arrays. However, the fabrication costs can be significant. Recently, the solution synthesis of ZnO nanorod arrays has been demonstrated as a simple, low temperature, and low-cost method [13–16]. Vertically aligned ZnO nanorod arrays have been used to produce AR layers [17,18]. Most of the research presented good AR properties with ZnO nanorod arrays. However, there is no report on the fabrication, nor tests of the properties of the real Si P–N junction solar cell devices incorporated with the ZnO nanorod arrays as the AR layers. In this paper, we report the effects of highly textured ZnO nanorod arrays, fabricated by low-temperature solution growth, on AR layer performance and apply them on the silicon solar cell to provide a promising technique for the fabrication of high-efficiency solar cell.

2. Experimental section

The ZnO nanorods used in the present experiment were grown on Si substrate and poly-Si solar cell by aqueous chemical growth method [13,16]. Before the growth process, the substrates were coated with a ZnO nanoparticle layer by the sol–gel preparation [19] as the seeding layer.

In this work, the poly-Si solar cells were fabricated on boron-doped poly-Si substrates with a thickness of 200 μm. The substrate surface was first roughened by the HF/HNO_3 solution to increase the illumination area. It was then doped to n-type with a Centrothem E-2000 APCVD to fabricate the P–N junction. The ion implanting depth was 80 nm. After the dopant activation, the

* Corresponding author.
E-mail address: kwsun@mail.nctu.edu.tw (K.W. Sun).

0927-0248/$ - see front matter © 2010 Elsevier B.V. All rights reserved.
doi:10.1016/j.solmat.2010.01.005

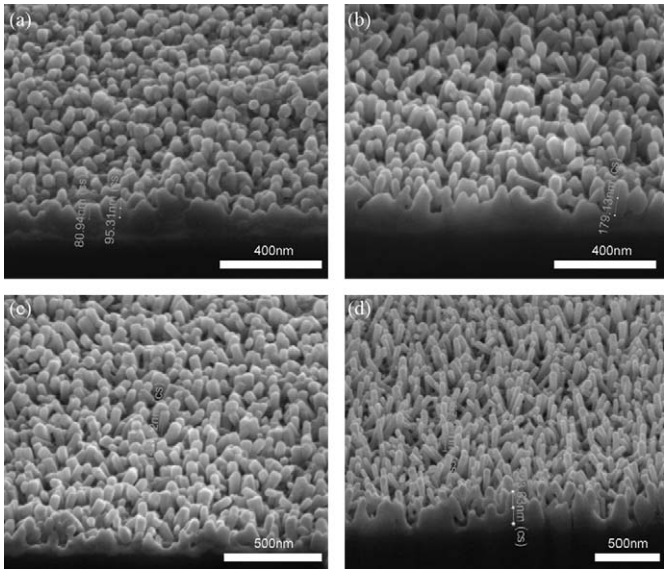

Fig. 1. SEM images of the vertically aligned ZnO nanorod arrays on Si substrates with growth time of (a) 120, (b) 180, (c) 240, and (d) 300 min.

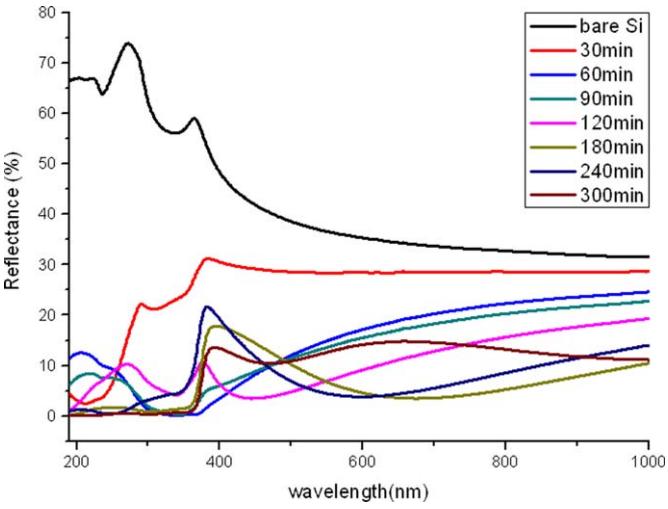

Fig. 2. Reflectance of the solution-grown ZnO nanorods with different growth time.

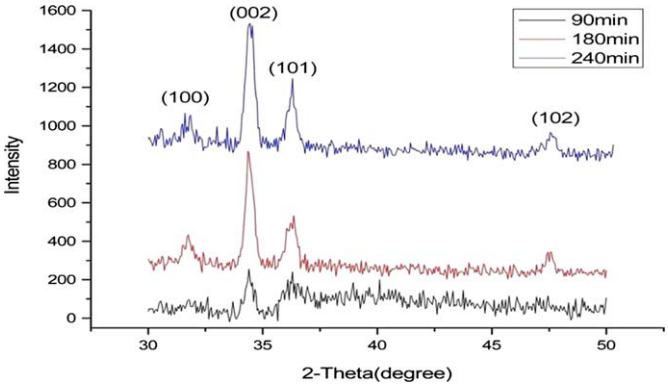

Fig. 3. X-ray diffraction patterns of ZnO nanorods with different growth time.

top and backside contacts were formed by a printer system (Baccini screen printing line) with Ag and Al. Finally, the cell was annealed at 850 °C to form ohmic contacts on both sides.

Both silicon wafers and poly-Si solar cells were used as the templates for the growth of the vertically aligned ZnO nanorod arrays. The substrate surface was first cleaned up with ACE, IPA, and D.I. water by ultrasonic agitation. The decomposition or hydrolysis of zinc salts is a well-established method to fabricate ZnO nanoparticle. First, the zinc acetate dihydrate and mono-ethanolamine were dissolved in the 2-methoxyethanol solution,

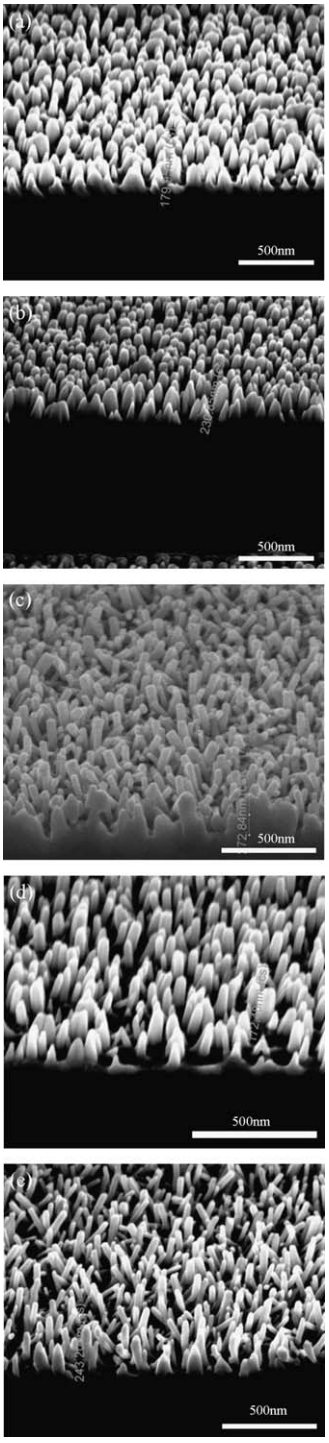

Fig. 4. SEM images of the vertically aligned ZnO nanorod arrays grown on Si substrates with spin-coating rate of (a) 1000, (b) 2000, (c) 3000, (d) 4000, and (e) 5000 rpm.

which served as the coating solution, at room temperature. The clean substrates were spin-coated with the solution at 1000–5000 rpm to ensure a uniform coverage of seeds and then the substrates were heated at 300 °C in air atmosphere for 1 h to yield layers of ZnO seeds. The solution for growing the ZnO nanorods was prepared by mixing the zinc nitrate hexahydrate with hexamethylenetetramine using the same molar concentration. The molar concentration was varied from 0.01 to 0.04 M. After the two solutions were mixed, the substrates were immersed inside the solution at 90 °C for 120–300 min. After the growth process was completed, the substrates were cleaned in D.I. water to remove the residual salt and amino complex and finally dried in air.

The surface morphology of the samples and size distribution of the vertically aligned ZnO nanorod arrays were characterized by scanning electron microscope (SEM) and X-ray diffraction (XRD). The reflection spectra of the samples were measured by an n&k analyzer (n&k Technology, Inc./n&k Analyzer 1280) for wavelengths ranging from 190 to 1000 nm. The poly-Si solar cell was characterized under the air mass 1.5 global (AM 1.5G) illumination condition.

3. Results and discussion

The geometries of the as-grown ZnO nanorods were tunable to varying degrees by changing the growth time, seed density, and solution composition. Here, we first compared the different AR performances of the controlled ZnO nanorod morphology on Si substrates.

Fig. 1 shows the SEM images of the vertically aligned ZnO nanorod arrays on Si substrates with growth time of 120, 180, 240, and 300 min when the growth solution with a molar concentration 0.02 M was used. The arrays consisted of nanorods with diameters of 50–60 nm and the lengths of the rods increased from ~80 to 320 nm as the growth time was increased. In Fig. 2, the reflectance spectra and the comparisons of AR performance of the above vertically aligned ZnO nanorod arrays with bare Si are shown. The figure shows that the ZnO nanorods with growth time of 180 min gave the lowest average reflection throughout the visible range among the others, and the reflectance was about 3%–4% at the wavelength of 667 nm. The increase in reflection as the growth time reached 300 min may be due to the larger inclined angles of the rods.

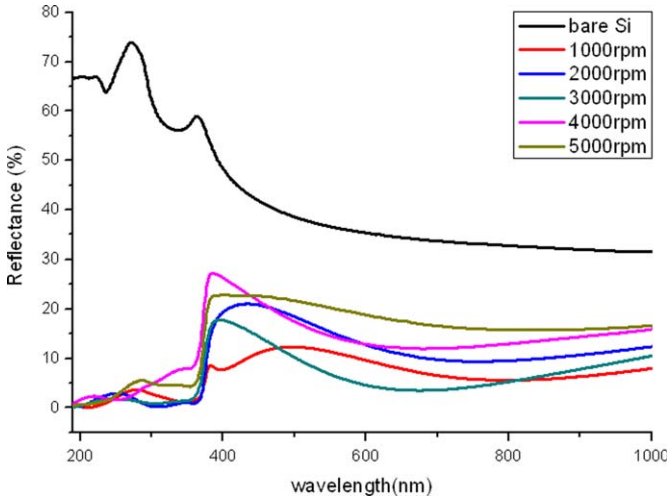

Fig. 5. Reflectance of the solution-grown ZnO nanorod with different spin-coating rate.

The X-ray diffraction (XRD) patterns of the ZnO nanorods with different growth time are illustrated in Fig. 3. Three pronounced wurtzite ZnO diffraction peaks (1 0 0), (0 0 2), and (1 0 1) appear at 2θ=31.89°, 34.65°, and 36.3°[15]. The XRD spectra of all ZnO nanorods revealed a strong (0 0 2) peak, indicating that the nanorods have high orientation with *c*-axis vertical to the substrate surface.

In the following we study the effects of the seed density on the reflection properties of the ZnO nanorods. The zinc acetate solution spin coating rotation rates were varied from 1000 to 5000 rpm and at a fixed growth time of 180 min. As shown in Fig. 4, the densities of ZnO nanorod arrays decreased from $3.2\times10^{10}\,\mathrm{cm}^{-2}$ to $1.2\times10^{10}\,\mathrm{cm}^{-2}$ as the rotation rates were increased from 1000 to 5000 rpm. Fig. 5 shows the reflectance spectra of the AR performances of the ZnO nanorod arrays with

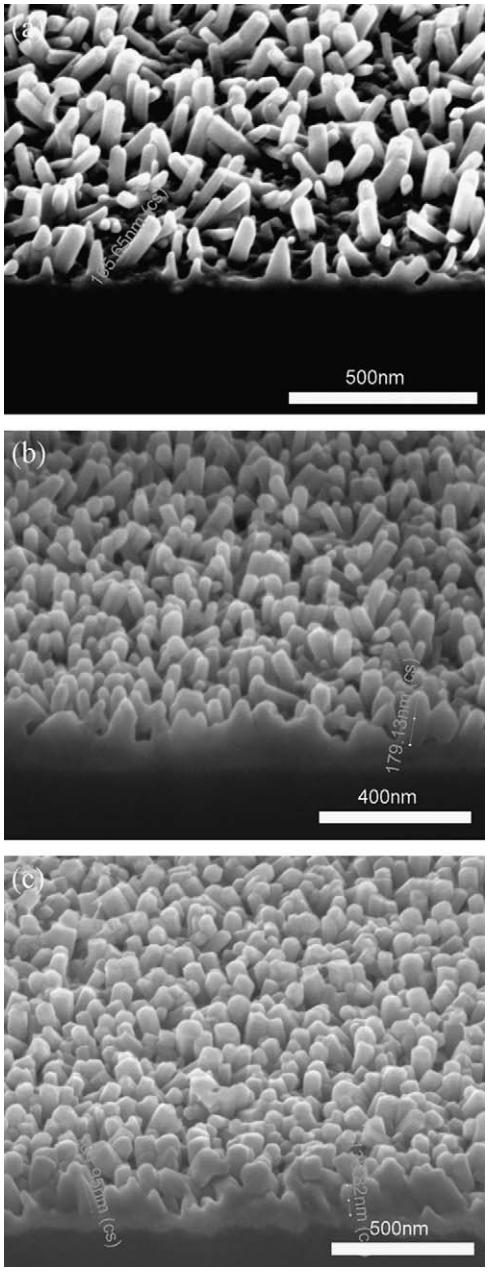

Fig. 6. SEM images of the vertically aligned ZnO nanorod arrays on Si substrates with growth solution concentration of (a) 0.01, (b) 0.02, and (c) 0.04 M.

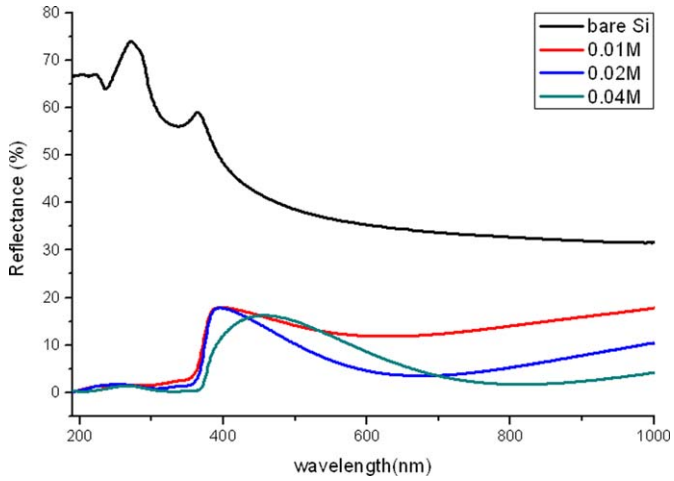

Fig. 7. Reflectance of the solution-grown ZnO nanorod with different growth solution concentration.

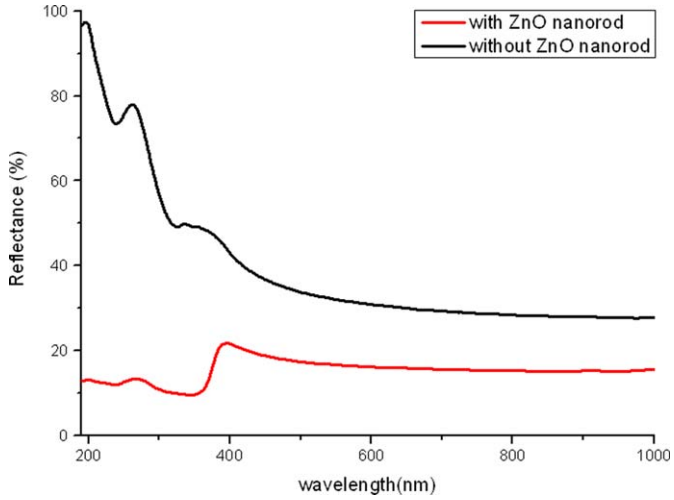

Fig. 8. Reflectance of the solar cell devices with the AR layer of ZnO nanorod arrays.

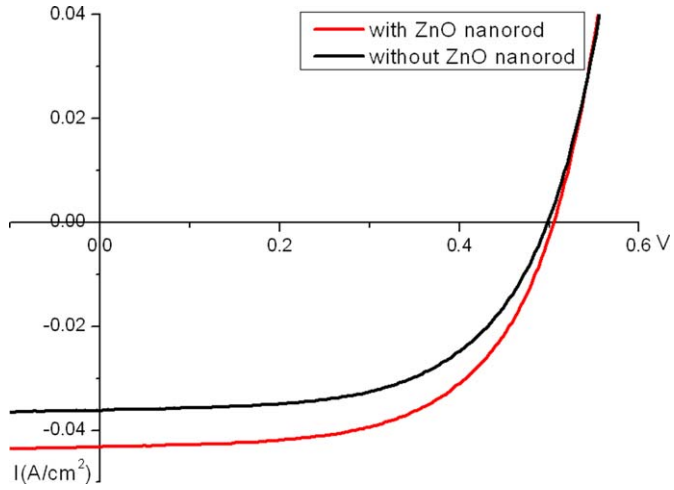

Fig. 9. *I–V* characteristics of the solar cells with and without the AR layers.

different nanorod densities and the comparisons with bare Si. We found that the nanorods fabricated with a moderate density at a spin coating rotation rate of 3000 rpm had the lowest average reflection throughout the visible range.

To compare the growth results at different growth solution concentrations, we experimented on solution concentrations ranging from 0.01, 0.02, to 0.04 M with a fixed spin coating rotation rate of 3000 rpm and growth time of 180 min. As shown in Fig. 6, the densities of ZnO nanorod arrays did not change as the solution concentrations were varied. However, the diameters of the nanorods increased to ~70–80 nm at the concentration of 0.04 M compared to 50–60 nm at the concentration of 0.01 M. Fig. 7 shows the reflectance spectra with different growth concentrations, in which the rods made with a solution concentration of 0.04 M show the lowest average reflection throughout the visible range.

From the above, we have demonstrated that the variations in growth conditions strongly influenced the morphology of the textured ZnO nanorods and had a great effect on the AR layer performance because of the differences in lengths, densities, and diameters of the nanorods. Finally, we demonstrated the growth of the ZnO nanorod arrays on the poly-Si solar cell as the AR layer using the optimized growth parameters of 180 min growth time, 5000 rpm spin coating rotation rate, and a solution concentration of 0.04 M. Comparisons of the resulting reflectance spectra from the ZnO nanorod AR layer with the bare poly-Si solar cell are shown in Fig. 8. The figure shows that the reflectivity is greatly reduced with the ZnO nanorod arrays. The poly-Si solar cell with ZnO nanorods was characterized under the air mass 1.5 global (AM 1.5G) illumination condition and was compared to the cell that did not undergo the AR treatment. The measured current–voltage characteristics are shown in Fig. 9. The short-circuit current was enhanced by 20% due to the presence of the ZnO nanorod layer. The light conversion efficiency of the solar cells was improved from 10.4% to 12.8% with the use of aligned ZnO nanorod arrays as the AR layer.

4. Conclusions

In summary, by using low-temperature solution growth, we showed a simple and low-cost method to produce vertically aligned ZnO nanorod arrays as AR layer. The structures can reduce surface Fresnel reflection over a broad spectral range. This technology was used for AR applications in solar cells to improve their light conversion efficiency. The light harvest efficiency of the poly-Si solar cells was improved by over 23% with the AR layers. It can find applications in other electro-optical devices.

Acknowledgement

This work was supported by the National Science Council of the Republic of China under contract No. NSC 96-2112-M-009-024-MY3, NSC 96-2120-M-009-004-, and the MOE ATU program.

References

[1] M. Ishimori, Y. Kanamori, M. Sasaki, K. Hane, Subwavelength antireflection gratings for light emitting diodes and photodiodes fabricated by fast atom beam etching, Jpn. J. Appl. Phys. 41 (2002) 4346–4349.
[2] Y. Kanamori, M. Sasaki, K. Hane, Broadband antireflection gratings fabricated upon silicon substrates, Opt. Lett. 24 (1999) 1422–1424.
[3] K. Hadobas, S. Kirsch, A. Carl, M. Acet, E.F. Wassermann, Reflection properties of nanostructure-arrayed silicon surfaces, Nanotechnology 11 (2000) 161–164.
[4] S. Wang, X.Z. Yu, H.T. Fan, Simple lithographic approach for subwavelength structure antireflection, Appl. Phys. Lett. 91 (2007) 061105 (3 pp).
[5] G.-R. Lin, Y.-C. Chang, E.-S. Liu, H.-C. Kuo, H.-S. Lin, Low refractive index Si nanopillars on Si substrate, Appl. Phys. Lett. 90 (2007) 181923 (3 pp).

[6] C.-H. Sun, W.-L. Min, N.C. Linn, P. Jiang, B. Jiang, Templated fabrication of large area subwavelength antireflection gratings on silicon, Appl. Phys. Lett. 91 (2007) 231105 (3 pp).
[7] C.-H. Sun, P. Jiang, B. Jiang, Broadband moth-eye antireflection coatings on silicon, Appl. Phys. Lett. 92 (2008) 061112 (3 pp).
[8] M.-L. Kuo, D.J. Poxson, Y.S. Kim, F.W. Mont, J.K. Kim, E.F. Schubert, S.-Y. Lin, Realization of a near-perfect antireflection coating for silicon solar energy utilization, Opt. Lett. 33 (2008) 2527–2529.
[9] P. Yu, C.-H. Chang, C.-H. Chiu, C.-S. Yang, J.-C. Yu, H.-C. Kuo, S.-H. Hsu, Y.-C. Chang, Efficiency enhancement of GaAs photovoltaics employing antireflective indium tin oxide nanocolumns, Adv. Mater. 21 (2009) 1618–1621.
[10] Mitsuhisa Kawakami, Agung Budi Hartanto, Yoshiki NakataTatsuo Okada, Synthesis of ZnO nanorods by nanoparticle assisted pulsed-laser deposition, Jpn. J. Appl. Phys. 42 (2003) L33–L35.
[11] Kwang-Sik Kim, Hyoun Woo Kim, Synthesis of ZnO nanorod on bare Si substrate using metal organic chemical vapor deposition, Phys. B 328 (2003) 368–371.
[12] R. Liu, A.A. Vertegel, E.W. Bohannan, T.A. Sorenson, J.A. Switzer, Epitaxial electrodeposition of zinc oxide nanopillars on single-crystal gold, Chem. Mater. 13 (2001) 508–512.
[13] Lori E. Greene, Matt Law, Dawud H. Tan, Max Montano, Josh Goldberger, Gabor Somorjai, Peidong Yang, General route to vertical ZnO nanowire arrays using textured ZnO seeds, Nano Lett. 5 (2005) 1231–1236.
[14] Youngjo Tak, Kijung Yong, Controlled growth of well-aligned ZnO nanorod array using a novel solution method, J. Phys. Chem. B 109 (2005) 19263–19269.
[15] Zhitao Chen, Lian Gao, A facile route to ZnO nanorod arrays using wet chemical method, J. Cryst. Growth (2006) 522–527.
[16] M. Riaz, A. Fulati, G. Amin, N.H. Alvi, O. Nur, M. Willander, Buckling and elastic stability of vertical ZnO nanotubes and nanorods, J. Appl. Phys. 106 (2009) 034309-1–034309-6.
[17] Y.J. Lee, D.S. Ruby, D.W. Peters, B.B. McKenzie, J.W.P. Hsu, ZnO nanostructures as efficient antireflection layers in solar cells, Nano. Lett. 8 (2008) 1501–1505.
[18] T.H. Ghong, Y.D. Kim, E. Ahn, E. Yoon, S.J. An, G.-C. Yi, Application of spectral reflectance to the monitoring of ZnO nanorod growth, Appl. Surf. Sci. 255 (2008) 746–748.
[19] Masashi Ohyama, Hiromitsu Kozuka, Toshinobu Yoko, Sol–gel preparation of ZnO films with extremely preferred orientation along (0 0 2) plane from zinc acetate solution, Thin Solid Films 306 (1997) 78–85.